arXiv:cond-mat/0407672v1 [cond-mat.mes-hall] 26 Jul 2004

Determination of the Intershell Conductance in Multiwalled Carbon Nanotubes

B. Bourlon,[1] C. Miko,[2] L. Forró,[2] D.C. Glattli,[1,3] A. Bachtold[1*]
[1] *Laboratoire Pierre Aigrain, Ecole Normale Supérieure,*
24 rue Lhomond, 75231 Paris 05, France. [2] *EPFL, CH-1015, Lausanne,*
Switzerland. [3] *SPEC, CEA Saclay, F-91191 Gif-sur-Yvette, France.*
(Dated: February 2, 2008)

We report on the intershell electron transport in multiwalled carbon nanotubes (MWNT). To do this, local and nonlocal four-point measurements are used to study the current path through the different shells of a MWNT. For short electrode separations $\lesssim 1$ μm the current mainly flows through the two outer shells, described by a resistive transmission line with an intershell conductance per length of $\sim(10\ \mathrm{k}\Omega)^{-1}/\mu$m. The intershell transport is tunnel-type and the transmission is consistent with the estimate based on the overlap between π-orbitals of neighboring shells.

PACS numbers: 73.63.Fg, 73.40.Gk, 73.23.-b, 72.80.Rj

The specific geometry of MWNTs that consist of several nested cylindrical graphene shells (Fig. 1(a)) has motivated intense work to understand their mechanic and electronic properties [1]. MWNTs are found to conduct charges exceptionally well with a conductivity better [2] or comparable [3] to that of low-resistivity metals. This high conductivity is attributed to the low level of diffusion experienced by conducting modes along the shells. These modes are characterized by long wavelengths in the circumference direction (Fig. 1(b)) as predicted from the electronic structure calculation, which is based on the delocalisation of π-orbital states along the shell surface (Fig. 1(c)).

In MWNTs, neighboring shells are most often incommensurate. The resulting lack of periodicity is expected to inhibit the charge delocalization in the radial direction. The intershell conduction is thus governed by hopping and depends on the π-orbital overlap of nearby shells (Fig. 1(c)). Therefore, the intershell conduction mechanism is thought to be significantly different compared to that in the sheet plane. However, the intershell resistance remains to be experimentally quantified.

As a first indication for the intershell resistance one could think of relying on the interlayer resistivity of pure graphite $\sim 10^{-5}$ Ωm. But, this value is ultra sensitive to the material quality and the interlayer separation, so that the resistivity is easily increased up to $\sim 10^{-3}$ Ωm [4, 5, 6, 7]. On the theoretical side, many groups have studied the intershell conduction but results differ dramatically depending on the model hypotheses [8, 9, 10, 11, 12, 13, 14, 15, 16]. For example, zero intershell transport is predicted for an infinitely long and perfect tube, since both the energy and the Bloch wave vector have to be conserved [11]. In contrast, it has been shown that the intershell transmission is large when electrons are injected as localized wave packets from outside the shell [10]. The attenuation length, which is the length necessary for a charge flowing along a shell to propagate into the next shell, was found to be very short $L_a \sim$1-10 nm [10]. Experimentally, some results indicating current anisotropy have been reported. It has been suggested that the current flows through one or a few of the outermost shells [2, 3] when the current is injected in the outer shell.

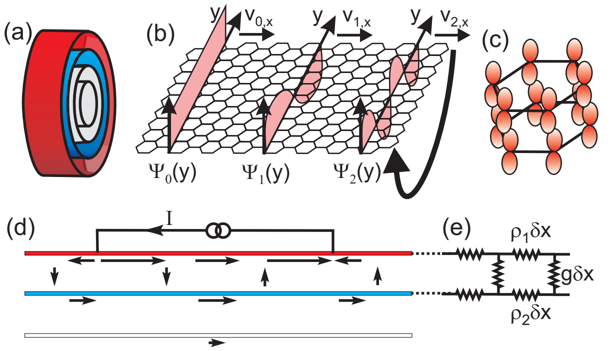

FIG. 1: (color online). Description of multiwalled nanotube. (a) A MWNT which consists of 4 shells. (b) A graphene sheet which gives a MWNT shell when rolled-up. Also shown is the slowly varying transverse part $\propto exp(ikr)$ of the electronic wave function. Ψ_0 corresponds to the two crossing subbands at the K point and Ψ_1 and Ψ_2 to the next successive subbands. (c) A hexagon of carbon π-orbitals. The two hexagons belong to two nearby incommensurate shells. The intershell resistance depends on the orbital overlap. (d) Current pathways. The 3 outermost shells are represented by lines of different colors. When current is externally applied, the current enters and exits the MWNT through the outermost shell. Importantly, part of I flows through to the second shell, so that the current pathway penetrates beside the region lying between the bias electrodes. (e) Resistive transmission line, which models the two outermost shells.

We report here a new method to access the electronic paths in MWNTs which enables the estimation of the linear intershell resistance. Using four-point measurement techniques, the voltage drop is measured between electrodes located inside or outside the region lying between the current biased electrodes. Surprisingly, a significant nonlocal voltage drop is observed. Such a result has been reported previously in a proceeding [17] and attributed to multiple shells conduction with the intershell electron pathways occurring near defects or tube end caps. We show here that the nonlocal voltage drop decreases exponentially with distance. Moreover, the local voltage measured in a standard four-probe configuration drops when the distance between the current electrodes is increased. These results are in agreement with a model which considers conduction through the two outermost shells and treats them as a resistive transmission line (Fig. 1(d,e)). In such a model, the intrashell resistance is $\sim$ 10 kΩ/μm and the intershell conductance is $\sim$(10 k$\Omega)^{-1}/\mu$m. This latter value is in agreement with the estimate based on electrons tunnelling through atomic orbitals of nearby shells while taking into account conservation of energy but not momentum. From this value, and the 0.34 nm intershell separation, we deduce a radial resistivity for MWNTs of $\sim$1 Ωm, much larger than that of bulk graphite.

We look first at the measurements of the nonlocal voltage $\Delta V_{nonlocal}$ (schematic of Fig. 2(a)). $\Delta V_{nonlocal}$ is linear with the applied current I at low bias. Such a finite nonlocal voltage at room temperature is a signature of systems possessing complex current pathways and is particularly evident in anisotropic materials such as high-temperature superconductors [18]. An example of current pathway is illustrated in Fig. 1(d). Interestingly, the values of the nonlocal resistance $\Delta V_{nonlocal}/I$ are comparable for all $\sim$ 40 studied MWNTs, which suggests similar current pathways for different MWNTs. Indeed, we get $V_{nonlocal}/I = 430\pm 90\ \Omega$ for devices with 400 nm electrode separations.

Now, we turn to the spatial dependence of the nonlocal voltage. For this purpose, 11 electrodes were attached on a single MWNT with about 20 shells. This allowed us to probe the $\Delta V_{nonlocal}$ dependence on the lengths x, L and d, where x is the separation between the voltage and current electrodes, L the separation between the current electrodes and d the separation between the voltage electrodes. Figure 2(a) shows that $\Delta V_{nonlocal}/I$ decreases exponentially with x with a decay length of 0.94 μm. We note that the current is zero far from the current electrodes such as at the tube end caps, showing that those play a negligible role in the current pathway. To verify this measurement, the voltage profile is measured along the tube with the farthest electrode taken as voltage reference (Fig. 2(b)). Again, the voltage decreases exponentially with a decay length equal to 0.92 μm.

When the separation L between the current biased electrodes is increased, $\Delta V_{nonlocal}$ gets larger as shown in Fig. 2(c). The spatial dependence is an exponential with a characteristic length of 0.94 μm. This measurement shows that more current is injected in inner shells for longer L. Indeed, only the current in the inner shells leads to current though the outermost shell in the nonlocal region (see Fig. 1(d)).

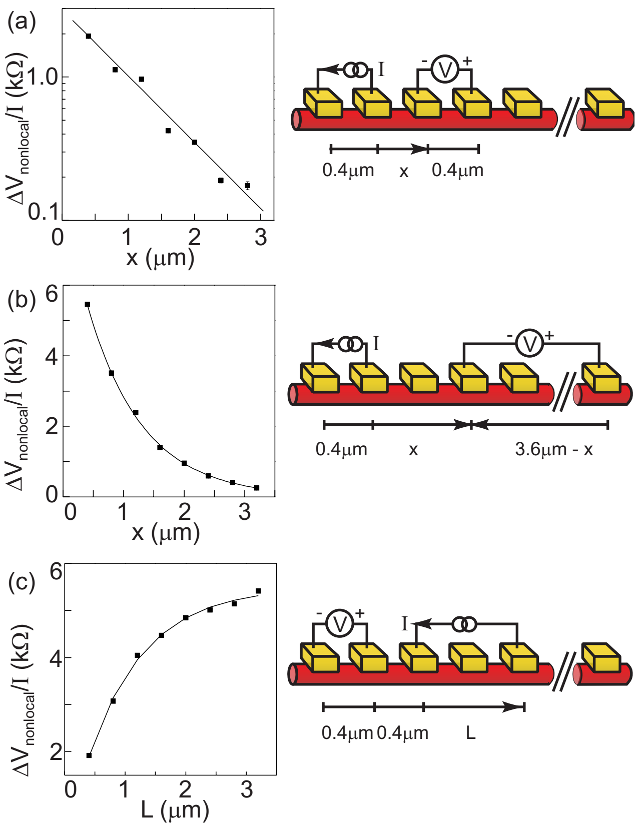

FIG. 2: (color online). Nonlocal voltage measurements on a MWNT electrically addressed by 11 electrodes. The schematics show the 5 μm long MWNT. The diameter is 17 nm, which corresponds to about 20 shells. The MWNT, synthesized by arc-discharge evaporation and carefully purified [29], was dispersed onto a 500 nm oxidized Si wafer from a dispersion in dichloroethane. Cr/Au electrodes were patterned above the tube by electron beam lithography. (a) $\Delta V_{nonlocal}$ as a function of the separation between the current and the voltage electrodes. $\Delta V_{nonlocal}/I$ is plotted on a logarithmic scale. The straight line corresponds to a decay length of 0.94 μm. Data are taken at 250 K. $\Delta V_{nonlocal}/I$ is measured in the linear regime with $eV = eIR_{2P}$ below kT, R_{2P} being the two-point resistance. (b) Nonlocal voltage as a function of the tube length. The voltage reference is taken at the extremity of the electrode series. The continuous curve is an exponential decay fit with a decay length of 0.92 μm. (c) $\Delta V_{nonlocal}$ as a function of the separation between the current electrodes. The continuous curve is proportional to $1 - exp(-L/L_a)$ with $L_a = 0.94$ μm.

We now turn our attention to the traditional four-point configuration with local voltage ΔV_{local} measurements. Fig. 3 shows that ΔV_{local} is not independent on L the distance between the current probes as would be expected for a standard four-point measurement, but instead ΔV_{local} increases as L is reduced. The spatial dependence is consistent with an exponential decay with a characteristic length of 2 μm, which is twice the value found above. This result points to the same finding as in the last paragraph, namely that the current injected into the inner shells increases with the separation between the current biased electrodes.

The current injection into the inner shells might be related to the electrodes. The MWNT structure could be modified by the process used for the fabrication of

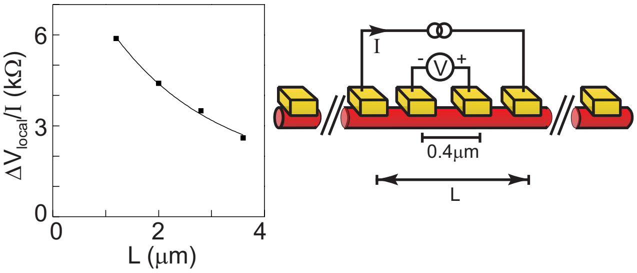

FIG. 3: (color online). Local voltage as a function of separation between the current biased electrodes. L is symmetrically increased with respect to the center between the voltage electrodes. The continuous curve is exponential with a decay length equal to 2 μm.

electrodes on top of the tube. However, measurements using a different device configuration, where the MWNT was deposited on top of existing electrodes, give similar results. This suggests that the fabrication process does not result in any MWNT damage that modifies its transport properties. An alternative effect related to electrodes might be that their presence is at the origin of the length dependence of ΔV_{local} and $\Delta V_{nonlocal}$. Indeed, the decay length is comparable to the electrode separation. To control for this effect, devices were fabricated with 6 electrodes separated by 400 nm except between the fourth and the fifth electrodes that were separated by 1100 nm. The two middle electrodes are current biased. The $\Delta V_{nonlocal}$ measured at x =400 nm is lower than that measured at x =1100 nm with a ratio consistent with measurements on MWNTs contacted by electrodes separated always by 400 nm. Therefore, the observed exponential dependences are an intrinsic property of the MWNTs we study. In addition, the metal electrodes do not provide additional pathways for the current to flow, short-circuiting the outer shell. Indeed, $\Delta V_{nonlocal}/I$ is observed to not depend on a low or large transmission at the contacts [19].

We discuss now the number of current carrying shells. The nonlocal voltage on the outermost shell is seen to decay exponentially on the scale of a micron. Thus, a fraction of the current leaves the outermost shell to penetrate into the inner shells over a typical length scale of $L_a \sim 1$ μm. The same phenomenon is expected to occur between the second shell and deeper shells. Due to the exponential dependence, only a small fraction of the current is thus expected to reach the third and the deeper shells when the separation between the current bias electrodes is lower than $\sim 1\mu$m.

Now, we consider a model based on a resistive transmission line for a quantitative analysis of the results (Fig. 1(e)). On a δx length, the intershell conductance is $g\delta x$ and the intrashell resistances are $\rho_1\delta x$ and $\rho_2\delta x$. For an infinite long MWNT, it gives

$$\frac{\Delta V_{nonlocal}}{I} = \frac{g\rho_1^2 L_a^3}{2}\exp(\frac{-x}{L_a}) \cdot \left(1-\exp(\frac{-d}{L_a})\right)\left(1-\exp(\frac{-L}{L_a})\right) \tag{1}$$

$$\frac{\Delta V_{local}}{I} = g\rho_1 L_a^3\left(\frac{\rho_2 d}{L_a} + 2\rho_1 \mathrm{sh}(\frac{d}{2L_a})\exp(\frac{-L}{2L_a})\right) \tag{2}$$

with $L_a^{-1} = \sqrt{g(\rho_1+\rho_2)}$. Equation (1) predicts an exponential form of $\Delta V_{nonlocal}/I$ as a function of x and L with the same characteristic length L_a, in excellent agreement with experiments. $\Delta V_{local}/I$ is expected in equation (2) to depend exponentially on L, this time with a characteristic length $2L_a$, which agrees again with experiments.

We estimate here ρ_1, ρ_2 and g by taking L_a =0.93 μm and comparing equations (1,2) to the measured values of $\Delta V_{nonlocal}/I$ for $x = L = d$ =0.4 μm and $\Delta V_{local}/I$ for $d = L/3$ =0.4 μm. However, $\Delta V_{nonlocal}/I$ or $\Delta V_{local}/I$ are not constant for different sections of the tube. These variations are attributed to local inhomogeneities in the electronic diffusion along the shell and/or to the imprecision in x, L and d due to the finite width 200 nm of the electrodes. Indeed, the electron transmission is probably non uniform along the tube/electrode interface and occurs at one or a few more preferential places. For a more accurate determination, we average over the 8 independent measurements obtained by translating the set of active probes by one unit each time. We get $\Delta V_{nonlocal}/I$ =780±170 Ω and $\Delta V_{local}/I$ =4.8±0.4 kΩ. This gives ρ_1 ~22 kΩ/μm, ρ_2 ~1 kΩ/μm and g ~(20 kΩ)$^{-1}$/μm. Taking these values and assuming the resistivity of the third shell $\rho_3 = \rho_2$, we estimate the transport contribution of the third shell to be less than 10% for a length shorter than 5 μm. This supports the double shell conduction analysis used here.

The same analysis is made for 8 different MWNTs which are 6-23 nm thick and which are connected by at least 7 electrodes. We obtain L_a =0.4-1 μm, ρ_1 =6-25 kΩ/μm, ρ_2 =0.05-2ρ_1 and g = (3.7-20 kΩ)$^{-1}$/μm. We note that ρ_1 is consistent with the MWNT resistance per length previously obtained [20]. In addition, the estimate for ρ_2 is very sensitive to variations of $\Delta V_{nonlocal}/I$ and $\Delta V_{local}/I$. However, ρ_2 is most often found lower than ρ_1, which suggests stronger diffusion in the outermost shell than in deeper shells. A possible explanation is that inner shells are protected by the outermost shell, which may be in direct contact with some adsorbed molecules or which may have been degraded during manipulation.

The intershell conductivity g ~(10 kΩ)$^{-1}$/μm is relatively large, when compared to most theoretical expectations [8, 9, 10, 11, 12, 13, 14, 15, 16]. As for the dependence on temperature T, Fig. 4(a) shows a weak variation $\Delta V_{nonlocal}/I$ versus T above 10 K, which suggests that the intershell conduction is not thermally activated. At lower temperatures, quantum effects appear as

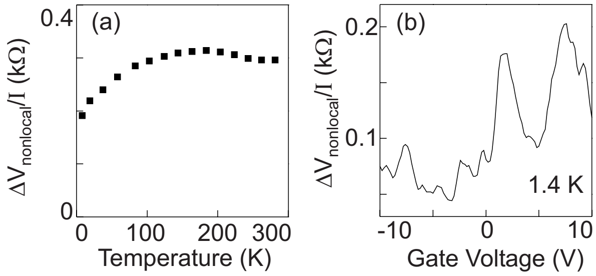

FIG. 4: Nonlocal voltage at low temperature. (a) $\Delta V_{nonlocal}$ as a function of temperature measured from 8 to 280 K. The MWNT diameter is 7 nm and the electrode separations are 450 nm. $\Delta V_{nonlocal}$ is averaged over the gate voltage. (b) $\Delta V_{nonlocal}$ as a function of gate voltage.

seen in the sensitivity of $\Delta V_{nonlocal}/I$ to a gate voltage which may be attributed to electronic interference and/or Coulomb interaction [21] (Fig. 4(b)). Importantly, the nonlocal voltage is well above zero showing that the intershell transmission is far from being blocked for T above 1.4 K.

The intershell conductance g is compared here to the predictions of tunnelling conductance G_{atom} through the π-orbital overlap between 2 atoms of nearby shells. Assuming elastic tunneling, G_{atom} is given by [22]

$$G_{atom} = \frac{4\pi e^2}{\hbar} N_{atom}^2 E_{bin}^2 \tag{3}$$

with E_{bin} the binding energy due to electronic delocalisation and $N_{atom} = \frac{2n}{hv_f}\frac{S}{2\pi r}$ the density of state per atom. $S = 2.6$ Å^2 is the surface occupied by one atom, r the shell radius, $v_f = 10^6$ ms^{-1} the Fermi velocity and $n =$ 10-20 the number of modes due to doping [23]. G_{atom} is related to g through $g = G_{atom}\frac{2\pi r}{S}$. Using $g = (10\ \text{k}\Omega)^{-1}/\mu$m, $n = 15$ and r=5 nm, we obtain that E_{bin} is on the order of 25 meV, in agreement with reported values for graphite. Indeed, the binding energy due to electronic delocalisation has been reported to contribute significantly to the interplanar cohesive energy, which has been theoretically estimated [24, 25] at $\sim$ 25 meV and measured [26] around $\sim$ 35 meV. We note that Eq. (3) gives a rather rough estimate for the intershell conduction. Indeed, G_{atom} is expected to be reduced due to shell incommensurability or Bloch wave vector conservation which is obeyed only partially because of disorder, finite tube length and tube deformation due the substrate roughness. On the other hand, the tube deformation can locally enhance the orbital overlap and thus g. However, a quantitative estimate of these effects is difficult at this stage.

The measure of the intershell conductance represents an important step in the characterisation of basic MWNT properties. We have found that the intershell conductance is largely independent of temperature and is consistent with tunnelling through orbitals of nearby shells. We have also shown that the current flows mainly along individual shells that are rather efficiently insulated from each other in spite of the short 0.3 nm shell separation. The control of charge pathways on the angstrom scale is obviously promising for future experiments or applications. For example, the effect on transport of the Coulomb interaction between neighbouring shells can be studied. It is also possible to fabricate an intramolecular field-effect transistor based on engineered MWNTs [27, 28] using a thin-diameter semiconducting shell that is gated by the next shell.

We thank B. Placais and C. Baroud for discussions and C. Delalande for support. LPA is CNRS-UMR8551 associated to Paris 6 and 7. The research has been supported by the DGA, ACN, sesame, the Swiss National Science Foundation and its NCCR "Nanoscale Science".

* corresponding author: bachtold@lpa.ens.fr

---

[1] C. Schonenberger, L. Forro, Phys. World **13**, 37 (2000).
[2] S. Frank *et al.*, Science **280**, 1744 (1998).
[3] A. Bachtold *et al.*, Nature **397**, 673 (1999).
[4] A.K. Dutta, Phys. Rev. **90**, 187 (1953).
[5] W. Primak, Phys. Rev. **103**, 544 (1956).
[6] C. Uher, L.M. Sander, Phys. Rev. B 27, 1326 (1983).
[7] K. Matsubara, K. Sugihara, T. Tsuzuku, Phys. Rev. B **41**, 969 (1990).
[8] S. Sanvito *et al.*, Phys. Rev. Lett. **84**, 1974, (2000).
[9] A.A. Maarouf, C.L. Kane, E.J. Mele, Phys. Rev. B **61**, 11156 (2000).
[10] S. Roche *et al.*, Phys. Rev. B **64**, R121401 (2001).
[11] Y.G. Yoon, P. Delaney, S. G. Louie, Phys. Rev. B **66**, 073407 (2002).
[12] D.H. Kim, K.J. Chang, Phys. Rev. B **66**, 155402 (2002).
[13] K.H. Ahn *et al.*, Phys. Rev. Lett. **90**, 026601 (2003).
[14] A. Hansson, S. Stafstrom, Phys. Rev. B **67**, 075406 (2003).
[15] S. Uryu, Phys. Rev. B **69**, 075402 (2004).
[16] F. Triozon *et al.*, Phys. Rev. B **69**, R121410 (2004).
[17] P.G. Collins *et al.*, *Proc. 14th Int. Winter School on Electronic Properties of Novel Materials* (Am. Inst. Phys., New York, 2000).
[18] R. Busch et al., Phys. Rev. Lett. **69**, 522 (1992).
[19] The contact resistance is roughly estimated by subtracting the four-point measurement from the two-point measurement, which varies from 5 kΩ to 3 MΩ for the MWNT of Fig. 2,3.
[20] A. Bachtold *et al.*, Phys. Rev. Lett. **84**, 6082 (2000).
[21] M.R. Buitelaar *et al.*, Phys. Rev. Lett. **88**, 156801 (2002).
[22] C.J. Chen, *Introduction to Scanning Tunnelling Microscopy* (Oxford University Press, 1993).
[23] M. Kruger *et al.*, Appl. Phys. Lett. **78**, 1291 (2001)
[24] M.C. Schabel, J.L. Martins, Phys. Rev. B **46**, 7185

(1992).
[25] J.C. Charlier, X. Gonze, J.P. Michenaud, Europhys. Lett. **28**, 403 (1994).
[26] L.X. Benedict *et al.*, Chem. Phys. Lett. **286**, 490 (1998).
[27] P. G. Collins, M. S. Arnold, Ph. Avouris, Science **292**, 706 (2001).
[28] B. Bourlon *et al.*, Phys. Rev. Lett. **92**, 026804 (2004).
[29] J.M. Bonard *et al.*, Adv. Mater. **9**, 827 (1997).